A CONVENIENT TOOL FOR STUDYING THE STABILITY OF PROTEINS AND NUCLEIC ACIDS
Differential scanning calorimetry

Concetta Giancola[*]

Department of Chemistry – University 'Federico II' of Naples, Via Cintia, Monte S.Angelo, 80126 Naples, Italy

The aim of this work is to discuss the thermodynamic properties, obtained by differential scanning calorimetry (DSC), of the thermal transition of proteins and nucleic acids and to analyze these data using statistical thermodynamic relations. The denaturation of the ordered, specific structures of biological macromolecules is a cooperative process and in many cases the macromolecules undergo a two-state transition. Differential scanning calorimetry, giving direct thermodynamic information, has proved to be very useful in clarifying the energetics of macromolecule transitions and in characterizing their thermal stability. Here, various examples are discussed: *i*) the equilibrium thermal denaturation of ribonuclease A, a model for the use of DSC by following the temperature-unfolding of the proteins, a monomolecular transition; *ii*) the equilibrium thermal dissociation of a DNA double helix in two strands, an example of how DSC is used to follow a bimolecular process; *iii*) an example of the use of DSC for studying the melting of unimolecular and tetramolecular DNA quadruple-helices.

Introduction

Differential scanning calorimetry is a useful technique to study the conformational transitions of biological macromolecules because it leads to the determination, in a single measurement, the temperature, the enthalpy and the heat capacity changes associated to the transition process. In particular, the enthalpy, being a thermodynamic potential, contains information on the states to which the system can belong within the investigated temperature range. Reviews on this methodology are available [1–8]. The principle of scanning microcalorimetry is to measure enthalpy changes of a solution of the macromolecules as a function of temperature change. This is obtained by measuring the power required to keep a sample at the same temperature as that of a reference solution as the temperature of both is increased in a linear manner. For biological solutions, the sample normally contains the macromolecule in buffer and the reference is the buffer solution. As the temperature changes, the macromolecule undergoes a transition in a cooperative fashion. This transition (protein denaturation or DNA dissociation) arises from the destruction of the numerous small forces that stabilize the native structure. Such disruption changes the enthalpy of the system giving rise to a drop in temperature, because the process is usually endothermic. The calorimeter will provide energy to the sample to maintain its temperature at the same value as that of the reference solution. The energy is measured as a power input and the raw output is a data set of power *vs.* temperature. Power is easily converted to the apparent molar excess heat capacity using the following equation:

$$<\Delta C_{\mathrm{P}}^{0}> = \frac{P}{\sigma m} \qquad (1)$$

where $<\Delta C_{\mathrm{P}}^{0}>$ is the apparent excess heat capacity in J mol^{-1} K^{-1}, P is power in J s^{-1}, σ is the scan rate in K s^{-1} and m is the number of moles of the protein in the sample. Thus, calorimetric curves (or profiles) are plots of $<\Delta C_{\mathrm{P}}^{0}>$ *vs.* temperature (see below).

Most small globular proteins show calorimetric profiles which can be represented by a two-state denaturation. In this case protein unfolding is readily represented by the following equilibrium equation:

$$K = \frac{[D]}{[N]} \qquad (2)$$

where K is the equilibrium constant for denaturation, $[N]$ represents the concentration of native form and $[D]$ the concentration of denatured protein. In these cases the thermodynamic parameters are simply derived and the thermodynamic analysis has a general applicability [9–13].

Pancreatic Ribonuclease A (RNase A) is one of the most thoroughly studied enzymes, and crystallographic structures have been determined in many laboratories [14]. The polypeptide chain contains

*   giancola@unina.it

124 residues and four disulfide bridges. The mechanism of folding was extensively studied by Wearne and Creighton [15], Udgaonkar and Baldwin [16], Rothwarf and Scheraga [17]. Thermal denaturation was followed calorimetrically by Privalov and Khechinashvili [9], Fujita and Noda [18], Barone and co-workers [19, 20]. RNase A denatures by a two-state mechanism.

Short DNA double helix segments also show calorimetric profiles which can be represented by a two-state denaturation. For these systems the term 'denaturation' should be replaced by the more appropriate term 'dissociation'. In fact, the thermodynamic properties of a short DNA duplex can be obtained by following, by micro-DSC, the dissociation of an ordered native structure (duplex) into the disordered, denatured state (single strands). The disruption of ordered regions of stacked base pairs in the DNA duplex can be measured by the change of excess heat capacity. The profile of excess heat capacity *vs.* temperature can be analyzed to yield quantitative thermodynamic data. Thermodynamic analyses derived from DNA dissociation helped to understand the sequence dependence in the secondary structure of nucleic acids [21–23].

In these last years there has been an increasing interest in quadruple-helix structures of DNA. The guanine (G) quadruplex motif is among the most interesting unusual conformation that DNA can adopt. DNA sequences with stretches of guanine residues that are capable of forming this four-stranded structure occur at the telomeric ends of eukaryotic chromosomes [24–27]. The capability of telomeric DNA sequences to adopt this unusual DNA conformation renders them particularly attractive as a target in anti-cancer therapy [28]. On the other hand, G-quadruplexes are also important because they have been implemented in the design of novel aptamers aimed at binding and inhibiting particular proteins [29–31]. For example, the sequence $^{5'}GGTTGGTGTGGTTGG^3$ (TBA: thrombin binding aptamer) is a strong anticoagulant in vitro, and inhibits the thrombin-catalyzed activation of fibrinogen [32, 33].

DSC is a convenient tool to study unimolecular quadruplex and can be utilized to study quadruplexes of any molecularity providing direct information on enthalpy changes of dissociations.

Experimental

Sample preparation

Ribonuclease A, type XII A, from bovine pancreas was purchased from Sigma as a lyophilized powder and was used without further purification. The protein was dissolved in 0.1 M sodium acetate buffer (pH 5.0), and dialyzed against the buffer solution. The final concentration of RNase A was determined by absorption spectroscopy using the extinction coefficient $A_{278}^{0.1\%}=0.71$ [34].

The oligonucleotides were synthesized using the phosphoramidite method [35]. The double helix was made up of two palindromic strands. The sequence of each strand is: $^{3'}$-d(AAGAGAAGGAAGCTTCCTTCTCTT)$^{5'}$. The 24-mer double helix was dissolved in a buffer at pH 6.0, containing 5 mM potassium phosphate, 140 mM KCl and 5 mM MgCl$_2$. The sequence $^{5'}$GGTTGGTGTGGTTGG^3 of the unimolecular quadruplex (TBA) was dissolved in a buffer containing 10 mM potassium phosphate, KCl 70 mM, EDTA 0.2 mM at pH 7.0. The sequence of each strand of tetramolecular quadruplex was $^{3'}$-d(TGGGGT)$^{5'}$. The quadruplex was dissolved in a buffer containing 10 mM sodium phosphate, 200 mM NaCl, 0.1 mM EDTA at pH 7.0. The concentrations of nucleic acids were determined spectroscopically by measuring the absorbance at 260 nm and a temperature of 90°C where the DNA is completely dissociated in single strands. The molar extinction coefficients were calculated by a nearest neighbour model [36]. Sample and reference vessels were filled with macromolecule solution and buffer, respectively. Scanning runs from 20 to 80 or 100°C were done at a heating rate of 0.5°C min^{-1}. In the case of quadruplex dissociation the heating rates were in the range 0.3–1°C min^{-1}. The reversibility was checked by cooling the sample to 20°C and reheating it to 80 or 100°C.

Equipment

The experiments described below require a standard commercial differential scanning microcalorimeter, for use with biological macromolecules. Biological and pharmaceutical products are usually studied in diluted solutions. Consequently, the associated thermal effects are very low, so that for detecting these phenomena highly sensitive DSCs, called micro DSC, can be used. The Setaram micro DSC equipped with two closed steel vessels (850 µL) has been used in our laboratory and it is routinely used in other laboratories [37, 38]. The vessels are removable and can be easily cleaned. The calorimeter was interfaced to an IBM PC computer for automatic data collection and analysis using previously described software [39].
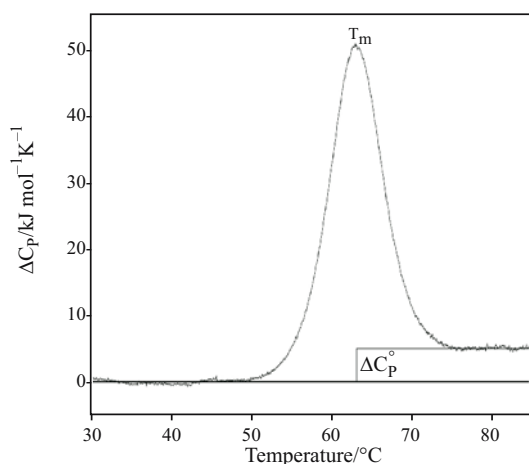
Fig. 1 Plot of the apparent excess heat capacity as a function of temperature for an endothermic process. The experimental transition enthalpy, $\Delta H^0(T_m)$, is obtained by integrating the area under the curve. T_m is the temperature at the maximum of the DSC peak. ΔC_P^0 is the difference between the denatured and native heat capacity values

Data analysis

A typical calorimetric curve reports the excess heat capacity function, $<\Delta C_p>$, *vs.* temperature (Fig. 1). The experimental transition enthalpy, $\Delta H^0(T_m)$, is obtained by integrating the area under the curve. T_m is the temperature corresponding to the maximum of DSC peak. ΔC_P^0 is the overall denaturation heat capacity, i.e. the difference between the denatured and native heat capacity.

For RNase A the van't Hoff enthalpy was calculated from the calorimetric data assuming as a preliminary hypothesis that a two-state N⇔D transition occurs [1]:

$$\Delta H_{v.H}^0 = \frac{4RT^2 \Delta C_P^0(T_m)}{\Delta H^0(T_m)} \qquad (3)$$

where $\Delta C_P^0(T_m)$ is the value of the excess heat capacity function at T_m, $\Delta H^0(T_m)$ is the calorimetric enthalpy and R is the gas constant. The calculated calorimetric to van't Hoff enthalpy ratio, $\Delta H^0(T_m)/\Delta H_{v.H}^0$ is unitary, which demonstrates that the RNase A denaturation is a two-state transition and $T_m=T_d$, the midpoint denaturation temperature. T_d is defined as the temperature at which 50% of the pro-

tein molecules are in the denatured state. Since RNase A denaturation at pH 5.0 is a reversible two-state transition, the equilibrium constant is unitary at T_d. Consequently, $\Delta G^0(T_d)=0$ and the denaturation entropy at T_d is simply calculated as:

$$\Delta S^0(T_d) = \frac{\Delta H^0(T_d)}{T_d} \qquad (4)$$

For the DNA double helix van't Hoff enthalpy was calculated by the calorimetric data assuming that a two-state $A_2 \Leftrightarrow 2A$ transition occurs [40]:

$$\Delta H_{v.H}^0 = \frac{6RT^2 \Delta C_P^0(T_m)}{\Delta H^0(T_m)} \qquad (5)$$

where $\Delta C_P^0(T_m)$, $\Delta H^0(T_m)$, T_m and R have the same significance as in Eq. (3) and the number 6 originates from the stoichiometry of the reaction.

Also in this case the $\Delta H^0(T_m)/\Delta H_{v.H}^0$ ratio is unitary, so that the dissociation is a reversible two-state process. As the dissociation depends on stoichiometry, it is necessary to calculate the entropy change with the following equation [41]:

$$\Delta S^0(T_m) = \frac{\Delta H^0(T_m)}{T_m} + R\ln Q \qquad (6)$$

where Q is the reaction quotient at T_m.

Results and discussion

RNase A denaturation

The thermodynamic parameters are reported in Table 1. These values agree well with the literature data [9, 18–20]. $\Delta H^0(T_d)$ and $\Delta S^0(T_d)$ are both positive. This is in agreement with a general picture of entropy driven denaturation process, while it is unfavourable by the enthalpic point of view. The observed endothermic $\Delta H^0(T_d)$ value results from endothermic contributions due to the intramolecular hydrogen bonds, as well as to hydrophobic and van der Waals interactions, and hydration effects. The positive $\Delta S^0(T_d)$ value is prevalently due to the higher conformational freedom of the protein in the denatured state. The ΔC_P^0 value is also positive and equal to 5.5 ± 0.2 kJ mol^{-1} K^{-1}. This positive value is due to the exposure to water of hydrophobic residues origi-

Table 1 Thermodynamic parameters for melting or dissociation processes

	$T_m/°C$	$\Delta H^0(T_m)$/kJ mol^{-1}	$\Delta S^0(T_m)$/kJ mol^{-1} K^{-1}	ΔG^0 (298)/kJ mol^{-1}
RNase A	61.3±0.1	465±10	1.39±0.05	39±1
24-mer DNA duplex	73.5±0.1	716±18	1.98±0.04	126±3
TBA quadruplex	53.1±0.1	91±5	0.26±0.02	13±1
d[TGGGGT]$_4$quadruplex	–	320±10	–	–

nally buried in the native structure according to current models [42–45 and reference therein].

Denaturation enthalpies, entropies and Gibbs energies can be calculated as a function of temperature by assuming that ΔC_P^0 is temperature independent, in a narrow temperature range. These thermodynamic functions can be obtained according to the well-known Kirkhhoff relationships:

$$\Delta H^0(T) = \Delta H^0(T_d) + \Delta C_P^0(T_d)(T - T_d) \qquad (7)$$

$$\Delta S^0(T) = \frac{\Delta H^0(T_d)}{T_d} + \Delta C_P^0(T_d) \ln \frac{T}{T_d} \qquad (8)$$

Finally, the free energy change can be calculated:

$$\Delta G^0(T) = \Delta H^0(T) - T\Delta S^0(T) \qquad (9)$$

A thermodynamic treatment of the two-state equilibrium leads to the calculation of the Gibbs energy difference between native and denatured state. This is done using the three experimental parameters: T_d, $\Delta H^0(T_d)$, ΔC_P^0. The ΔG^0 profiles as function of temperature (Fig. 2) are known as 'protein stability curves' [10].

Two intriguing features can be noted:

- The stability curves have the shape of a slightly skewed parabola that intersects the temperature axis in two points, corresponding to the so-called 'cold' and 'hot' denaturation temperature [46]. Many years ago Brandts theoretically anticipated the occurrence of a 'cold' denaturation [47, 48]. Then Privalov and co-workers observed the phenomenon by DSC when they analyzed the denaturation of met-myoglobin [49, 50].

- The stability of native structure is marginal: it amounts, on average, to 40–60 kJ mol^{-1} at room temperature. This quantity, when normalized per residue for proteins of 100–200 resi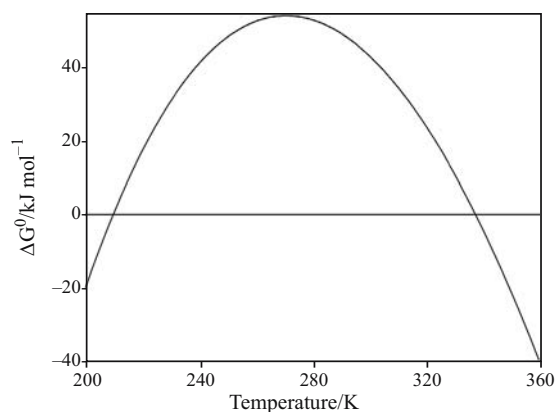dues, roughly corresponds to the molecular random thermal energy RT [51]. The marginal stability is related to the delicate interlocking between rigidity and flexibility required for proteins to perform their biological function. It arises from a subtle balance of large numbers of interactions corresponding to different stabilizing and destabilizing interactions above mentioned.

Data simulation of RNase A denaturation

Assuming that temperature-induced RNase A denaturation at pH 5.0 is a reversible two-state transition between the native, N, and denatured, D, state: $N \Leftrightarrow D$

The equilibrium constant, K, can be expressed as

$$K = \frac{[D]}{[N]} \qquad (10)$$

where $[N]$ and $[D]$ are the protein concentrations in its native and denatured states, respectively.

At any temperature f_D and f_N represent the fraction of molecules in the native and denatured state, respectively:

$$f_D = \frac{[D]}{[N] + [D]} = \frac{K}{1 + K} \qquad (11)$$

$$f_N = 1 - f_D = \frac{[N]}{[N] + [D]} = \frac{1}{1 + K} \qquad (12)$$

The molar Gibbs energy of denaturation, ΔG^0, can be obtained from the equilibrium constant as:

$$\Delta G^0 = -RT \ln K \qquad (13)$$

where R is the gas constant. The standard denaturation enthalpy follows directly from the Gibbs–Helmholtz relationship:

$$\left[\frac{\partial \left(\frac{\Delta G^0}{T} \right)}{\partial T} \right]_P = -\frac{\Delta H^0}{T^2} \qquad (14)$$

which can be further transformed, combining the two above equations, into the van't Hoff relation:

$$\left(\frac{\partial \ln K}{\partial T} \right)_P = \frac{\Delta H^0}{RT^2} \qquad (15)$$

The integrated form can be written as:

$$K(T) = \exp\left[\left(-\frac{\Delta H^0(T)}{R} \right) \left(\frac{1}{T} - \frac{1}{T_0} \right) \right] \qquad (16)$$

Assuming $T_0 = T_d$, the equation takes the form:

$$K(T) = \exp\left[\left(-\frac{\Delta H^0(T)}{R} \right) \left(\frac{1}{T} - \frac{1}{T_d} \right) \right] \qquad (17)$$

Fig. 2 Stability curve, ΔG^0 *vs. T*, for RNase A calculated by means of Eq. (9) by introducing the thermodynamic parameters of Table 1

At each temperature, the enthalpy of this thermodynamic system can be described as:

$$H(T)=f_N H_N + f_D H_D = H_N + f_D(H_D - H_N)=$$
$$=H_N + f_D \Delta H^0(T_d) \qquad (18)$$

where H_N and H_D are the enthalpy of native and denatured states, respectively.

Choosing the native state as the reference state, the following equation for the excess enthalpy is obtained:

$$<\Delta H^0(T)>=H(T)-H_N(T)=f_D \Delta H^0(T_d) \quad (19)$$

which can be derived with respect to the temperature:

$$<\Delta C_P^0(T)>=\frac{[\Delta H^0(T_d)]^2}{RT^2}\frac{K}{(1+K)^2}+\Delta C_P^0 \frac{K}{1+K} \quad (20)$$

The DSC curve of RNase A was simulated using Eq. (20). The good agreement between the one-step simulated transition and the experimental curve is shown in Fig. 3.

Dissociation of 24-mer DNA double helix

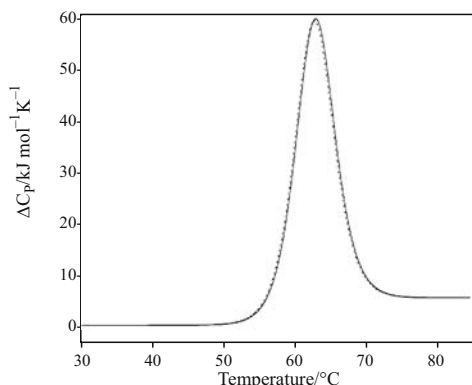The thermodynamic parameters of DNA melting, at pH 6.0 and $c=4.17\cdot10^{-5}$ M, are shown in Table 1.

Fig. 3 Superimposition of the experimental DSC curve of RNase A (solid line) with that calculated by means of Eq. (20) (broken line); $c=1.50\cdot10^{-4}$ M
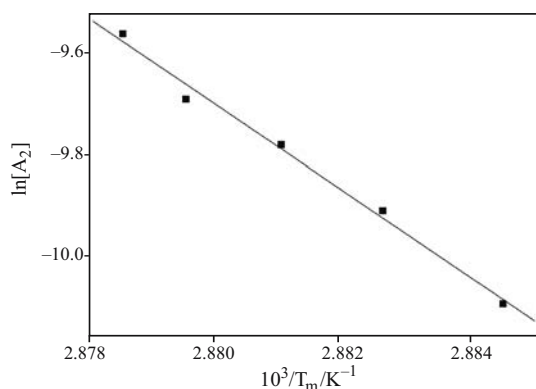

Fig. 4 van't Hoff plot of $\ln[A_2]$ *vs.* $1/T_m$ where $[A_2]$ is the double helix concentration and T_m is the melting temperature

Since the dissociation is a bimolecular process, the stability is influenced by the DNA duplex concentration and the maximum of the curve does not coincide with T_d ($T_m \neq T_d$) because T_m does not correspond to 50% of transition. The value of T_m increases as the concentration increases according to the following equation [52]:

$$\ln[A_2]=\text{constant}-\frac{\Delta H_{v.H}^0}{RT_m} \qquad (21)$$

The plot of $\ln[A_2]$ *vs.* $1/T_m$ is shown in Fig. 5. The value of the calculated van't Hoff enthalpy is 708 kJ mol^{-1}, in good agreement with the experimental value of 716 kJ mol^{-1} directly obtained by the area under the curve, and the value of 711 kJ mol^{-1} calculated by DSC profiles utilizing Eq. (5) [53]. These values normalized to the number of base pairs correspond to an enthalpy value of about 30 kJ mol^{-1}. Klump and Ackermann calculated a contribution of 7.5 and 15.1 kJ per mole of base pairs for one hydrogen bonds formation and for the stacking interaction, respectively [54]. Consequently, one base pair coupling contributes of about 30 kJ mol^{-1}, the same value found for the 24-mer dissociation enthalpy.
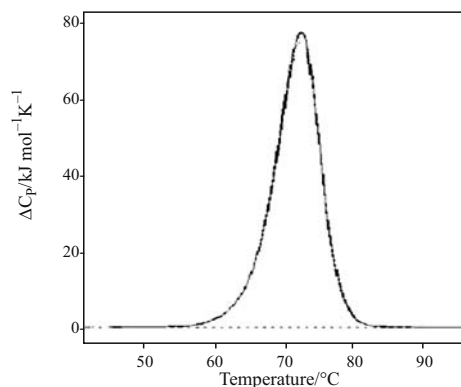

Fig. 5 Superimposition of the experimental DSC curve of the 24-mer DNA duplex (solid line) to that calculated by means of Eq. (25) (broken line); $c=4.17\cdot10^{-5}$ M

Data simulation of double helix dissociation

Starting from a palindrome double helix, A_2, the dissociation process is: $A_2 \Leftrightarrow 2A$.

The equilibrium constant can be expressed as:

$$K=\frac{[A]^2}{[A_2]} \text{ or } K=\frac{f_A^2}{f_{A_2}}C_t \qquad (22)$$

where $f_A=[A]/C_t$ and $f_{A_2}=[A_2]/C_t$ and C_t is the total duplex concentration. Considering the stoichiometry and the mass conservation the following equation holds at any temperature:

$$f_{A_2} + \frac{1}{2}f_A = 1 \qquad (23)$$

The solution of the Eqs (22) and (23) permits the determination of the excess enthalpy

$$<\Delta H> = (1 - f_{A_2})\Delta H^0 \qquad (24)$$

where ΔH^0 is the enthalpy change of the dissociation process.

The corresponding excess heat capacity, $<\Delta C_P>$, can be calculated by the numerical differentiation of Eq. (24):

$$<\Delta C_P^0> \left[\frac{\partial (<\Delta H^0>)}{\partial T} \right]_P \qquad (25)$$

At any temperature, the equilibrium constant has been determined according to the equation:

$$K(T) = K(T_m)e^{-\frac{\Delta H^0}{R}\left(\frac{1}{T} - \frac{1}{T_m}\right)} \qquad (26)$$

where $K(T_m)$ value is assumed equal to $2C_t$.

The calculated curve superimposed to the experimental data is shown in Fig. 5.

Dissociation of DNA quadruplexes

The calorimetric profile of the unimolecular quadruplex (TBA) is shown in Fig. 6a, and the thermodynamic parameters are collected in Table 1. The denaturation process is reversible and the DSC profile is not affected by either concentration or scan rate. The observed $\Delta H^0(T_m)$ value results prevalently from endothermic contributions due to the eight hydrogen bonds per tetrad, the stacking interactions between tetrad planes and the ions released from the quadruplex cavity. This value perfectly agrees with enthalpy values previously found [55–57], but it is smaller than the calculated $\Delta H_{v.H}$ value of 160 kJ mol^{-1} [56–58]. This discrepancy between calorimetric and calculated values $(\Delta H^0(T_m)/\Delta H^0_{v.H} < 1)$ could be due to a number of molecules not perfectly structured in their native state or to a partial aggregation phenomenon.

As for the dissociation of tetramolecular [d(TGGGGT)]$_4$ quadruplex, the melting temperature and the calorimetric profile are instead affected by the scan rate (Fig. 6b). This arises when the complexes are not at thermodynamic equilibrium during the temperature changes, and it is due to the slow rates of dissociation and/or association process. Consequently, the thermodynamic parameters cannot be obtained from DSC melting experiments and the calorimetric T_m values should be considered an upper limit. In these non-equilibrium conditions only the enthalpy change relative to the quadruplex dissociation process may be directly obtained from differential scanning
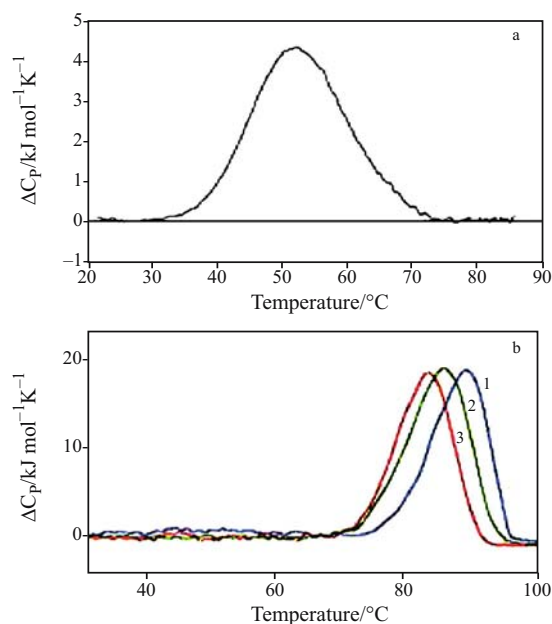

Fig. 6 Calorimetric heat capacity *vs.* temperature profiles for a – the TBA quadruplex ($c=5\cdot10^{-4}$ M), and b – the [TGGGGT]$_4$ quadruplex at a scan rate of 1.0 (1), 0.5 (2) and 0.3°C min^{-1} (3). Data were collected at $6.6\cdot10^{-4}$ M single strand concentrations

microcalorimetry measurements. The $\Delta H^0(T_m)$ value obtained for this quadruplex dissociation is 320 kJ mol^{-1}, corresponding to a value of 80 kJ mol^{-1} per tetrad, in good agreement with previously reported values for other quadruplexes [59–61].

Conclusions

DSC measurements offer the opportunity to perform careful physical measurements on biological macromolecules. They touch upon several key concepts involving the cooperativity of structural transitions, the intra- and inter-molecular forces determining the stability of macromolecules and the direct comparison between experimental and theoretical curves. In a single experiment, DSC directly measures and allows calculating all the thermodynamic parameters characterizing a biological macromolecule. Furthermore, it is the only technique that provides a direct measurement of enthalpy and heat capacity changes. Thus, DSC can be used to study the stability of any biological system, while combined with other biophysical methods offers the possibility to gather a whole spectrum of information on thermodynamics, structure, and function of biomolecules.

References

1 R. L. Biltonen and E. Freire, CRC Crit. Rev. Biochem., 5 (1978) 85.

2 P. L. Privalov, Adv. Protein Chem., 33 (1979) 167.

3 P. L. Privalov and S. A. Potekin, Methods Enzymol., 131 (1986) 4.

4 A. Cooper and C. M. Johnson, Methods Mol. Biol., 22 (1994) 125.

5 E. Freire, Methods Mol. Biol., 40 (1995) 191.

6 I. Jelesarov and H. R Bosshard, J. Mol. Recognit., 12 (1999) 3.

7 H.-J. Hinz and F. P. Schwarz, Pure Appl. Chem., 73 (2001) 745.

8 G.Bruylants, J. Wouters and C. Michaux, Curr. Med. Chem., 12 (2005) 2011.

9 P. L. Privalov and N. N. Khechinashvili, J. Mol. Biol., 86 (1974) 665.

10 W. J. Becktel and J. A. Schellman, Biopolymers, 26 (1987) 1859.

11 J.Sturtevant, Annu. Rev. Phys. Chem., 38 (1987) 463.

12 P. L. Privalov, Annu. Rev. Biophys. Biophys. Chem., 18 (1989) 47.

13 B. Chowdhry and S.Leharne, J. Chem. Educ., 74 (1997) 236.

14 A. Wlodawer in 'Biological Macromolecules and Assemblies' Vol. 2 of 'Nucleic acid and Interactive Proteins', F. A. Jurnak and A. McPherson (Eds), Wiley, New York 1985, p. 393.

15 S. J. Wearne and T. E. Creighton, Proteins: Struct., Funct. Genet., 4 (1988) 251.

16 J. B. Udgaonkar and R. L. Baldwin, Nature, 335 (1988) 694.

17 D. M. Rothwarf and H. A. Scheraga, J. Am. Chem. Soc., 113 (1991) 6293.

18 Y. Fujita and Y. Noda, Bull. Chem. Soc. Jpn., 57 (1984) 1891.

19 G. Barone, F. Catanzano, P. Del Vecchio, C. Giancola and G. Graziano, Pure. Appl. Chem., 69 (1997) 2307.

20 C. Giancola, P. Del Vecchio, C. De Lorenzo, R. Barone, R. Piccoli, G. D'Alessio and G. Barone, Biochemistry, 39 (2000) 7964.

21 G. Plum, Y. Park, S. Singleton, P. Dervan and K. Breslauer, Proc. Natl. Acad. Sci. USA, 87 (1990) 9436.

22 J. Puglisi and I. Tinoco, Methods Enzymol., 180 (1989) 304.

23 F. Aboul-ela, D. Koh, I. Tinoco and F. Matin, Nucl. Acids Res. 13 (1985) 4811.

24 Y. Wang and D. J. Patel, Structure, 1 (1993) 263.

25 Y. Wang and D. J. Patel, Structure, 2 (1994) 1141.

26 Y. Wang and D. J. Patel, J. Mol. Biol., 251 (1995) 76.

27 G. N. Parkinson, M. P Lee and S. Neidle, Nature, 417 (2002) 876.

28 J. L. Mergny, P. L. Maillet, F. Lavelle, J. F. Riou, A. Laoui and C. Helene, Anticancer Drug Des., 14 (1999) 327.

29 Y. Lin, A. Padmapriya, K. M. Morden and S. D. Jayasena, Proc. Natl. Acad. Sci. USA, 92 (1995) 11044.

30 Y. Lin and S.D. Jayasena. J. Mol. Biol., 271 (1997) 100.

31 J. D. Wen and D. M. Gray, Biochemistry, 41 (2002) 11438.

32 L. C. Griffin, G. F. Tidmarsh, L. C. Bock, J. J. Toole and L. L. Leung, Blood, 81 (1993) 3271.

33 W. X. Li, A. V. Kaplan, G. W. Grant,. J. J. Toole and L. L. Leung, Blood, 83 (1994) 677.

34 E. Freire and R. L. Biltonen, Biopolymers, 17 (1978) 463.

35 Oligonucleotide Synthesis: A Practical Approach, M. Gait, Ed., IRL Press, Oxford (1984).

36 C. R. Cantor, M. M Warshaw and H. Shapiro, Biopolymers, 9 (1970) 1059.

37 D. Fessas, M. Signorelli and A. Schiraldi, J. Therm. Anal. Cal., 82 (2005) 691.

38 M. F. M. Sciacca, D. Miliardi, M. Pappalardo, C. La Rosa and D. M. Grasso, J.Therm. Anal. Cal., 86 (2006) 311.

39 G. Barone, P. Del Vecchio, D. Fessas, C. Giancola and G. Graziano, J. Thermal Anal., 38 (1993) 2779.

40 K. J. Breslauer, in Thermodynamic Data for Biochemistry and Biotechnology, H. J. Hinz, Ed., Springer, Berlin 1986.

41 C. Giancola, A. Buono, L. De Napoli, D. Montesarchio, D. Palomba, G. Piccialli and G. Barone, J. Thermal Anal., 38 (1999) 1177.

42 K. P. Murphy and E. Freire, Adv. Protein Chem., 43 (1992) 313.

43 G. I. Makhatadze and P. L. Privalov, Adv. Protein Chem., 47 (1995) 307.

44 G.Barone, P. Del Vecchio, P. Giancola and G. Graziano, Int. J. Biol. Macromol., 17 (1995) 251.

45 H. Xu and K. Dill, J. Phys. Chem. B, 109 (2005) 23611.

46 P. Privalov, Crit. Rev. Biochem. Mol. Biol., 25 (1990) 281.

47 J. F. Brandts, J. Am. Chem. Soc., 86 (1964) 4291.

48 J. F. Brandts, Structure and Stability of Biological Macromolecules, S. N. Timascheff and G. D. Fasman, Eds, Dekker, New York 1969, p. 213.

49 P. L. Privalov, Yu. V. Griko, S. Yu. Venyaminov and V. P. Kutyshenko, J. Mol. Biol., 190 (1986) 487.

50 Yu. V. Griko, P. L. Privalov, J. M. Sturtevant and S. Yu. Venyaminov, Proc. Natl. Acad. Sci., 85 (1988) 3343.

51 M. Karplus and E. I. Shakhnovich, in 'Protein folding', Ed. T. E. Creighton, W. H. Freeman and Co., New York 1992, p. 127.

52 C. R. Cantor and P. R. Schimmel, in Biophysical Chemistry, Part III, Freeman, San Francisco 1980, p. 1201.

53 C. Giancola, A. Buono, D. Montesarchio and G. Barone, Phys. Chem. Chem. Phys., 1 (1999) 5045.

54 H. Klump and T. Ackermann, Biopolymers, 10 (1971) 513.

55 R. F. Macaya, P. Schultze, F. W. Smith, J. A. Rose and J. Feigon, Proc. Natl. Acad. Sci. USA, 90 (1993) 3745.

56 I. Smirnov and R. H. Shafer, Biochemistry, 39 (2000) 1462.

57 B. I. Kankia and L. A. Marky, J. Am. Chem. Soc., 123 (2001) 10799.

58 L. Martino, A. Virno, A. Randazzo, A. Virgilio, V. Esposito, C. Giancola, M. Bucci, G. Cirino and L. Mayol, Nucleic Acids Res., 34 (2006) 6653.

59 L. Petraccone, E. Erra, A. Galeone, A. Randazzo, A. Mayol, G. Barone and C. Giancola, Int. J. Biol. Macromol., 31 (2003) 131.

60 L. Petraccone, E. Erra, V. Esposito, A. Randazzo, A. Mayol, L. Nasti, G. Barone and C. Giancola, Biochemistry, 43 (2004) 4877.

61 J. L. Mergny, A. De Cian, S. Amrane and M. Webba da Silva, Nucleic Acids Res., 34 (2006) 2386.